View metadata, citation and similar papers at core.ac.uk
brought to you by CORE
provided by ScholarBank@NUS

Effect of shrinkage reducing admixture on flexural behaviors of fiber reinforced cementitious composites

Jun-Yan Wang[a,*], Nemkumar Banthia[b] and Min-Hong Zhang[a]

[a] *Department of Civil & Environmental Engineering, National University of Singapore, 1 Engineering Drive 2, Singapore 117576*

[b] *Department of Civil Engineering, University of British Columbia, 2024-6250 Applied Science Lane, Vancouver, BC, Canada V6T 1Z4*

ABSTRACT

The use of shrinkage reducing admixture (SRA) at various concentrations was investigated in fiber reinforced cementitious composites. Both mortar and high strength concrete (HSC) matrices were tested. Two types of fibers—steel and polypropylene—were assessed. The effect of SRA was measured on the fundamental properties such as surface tension of the bulk fluids and the contact angle developed between the fibers and the bulk fluids, on the fresh properties such as the air content and the density, and finally on the hardened mechanical properties, specially the flexural behaviors. It was noted that SRA enhances the wettability of fibers and reduces the air content of fiber reinforced cement mortars, while critical SRA concentrations are existing. SRA with critical concentration can significantly improve the flexural toughness and residual strength of steel fiber reinforced cement mortar. In the case of polypropylene fiber, SRA is not as effective in enhancing the flexural behaviors as it is in the case of steel fiber. SRA is generally ineffective in reducing the air content of HSC and the properties of steel fiber reinforced HSC with SRA are inferior to those without SRA.

[*] Corresponding author. Tel.: +65-9175 2275; Fax: +65-6779 1635.
Email address: johnsonong25@gmail.com (JY Wang)

Keywords: Shrinkage reducing admixture; surface tension; contact angle; fiber reinforced cement composite; flexural toughness; ASTM C1609

1. Introduction

The addition of fiber significantly improves not only the ductility [1,2], but also the durability of concrete [3]. The enhanced performance of fiber reinforced cement composite (FRC) compared to its unreinforced counterpart stems from its improved capacity to absorb energy during fracture, when properly designed fibers undergo pull-out processes, and the work needed for pull-out leads to significantly enhanced energy absorption capability [4]. This energy absorption attribute of FRC is often termed 'toughness'. A proper bonding between fiber and the cementitious matrix is critical in the context of an enhanced toughness. A properly engineered fiber-matrix bond will lead to a higher pull-out resistance over a large range of slip distances and thus enable the material to undergo large deflections while maintaining residual strength as much as possible and maintaining serviceability. Given the direct dependence of toughness and residual strength on the bond-slip response of fibers, significant number of studies have been carried out to understand and enhance such a response. Bond-slip characteristics of fibers embedded in cementitious matrices are known to be influenced by variables such as the rate of load application [5,6] temperature of the environment [6], fiber inclination [7], fiber surface modifications such as coatings, surface indentations and notches [8,9], addition of admixtures such as silica fume and metakaolin [10] and introduction of mechanical deformations [11].

As well known, the incorporation of fibers can introduce considerable amount of air in the mix, especially in the case of a cement mortar [12,13]. This part of air is usually entrapped in the matrix and can be as high as 10% by volume. The entrapped air is harmful in terms of the mechanical properties and adversely affects the durability.

Shrinkage reducing admixture (SRA) has been developed to reduce the surface tension of concrete's pore solution, thereby reducing the magnitude of capillary stresses and shrinkage strains that occur during hydration and when concrete loses moisture [14]. SRA also destabilizes air voids and allows them to be drained from concrete during the mixing process. This effect simultaneously contributes to the densification of interfacial transition zone between fiber and matrix and consequently leads to a stronger fiber-matrix bond [15].

In fiber reinforced concrete, the wettability of the fiber is often determined by the contact angle that the fiber develops with the mix water in its vicinity, which, in turn, determines whether the fiber is hydrophobic or hydrophilic. A lower contact angle signifies that the fiber is hydrophilic and will develop a denser transition zone around it with a stronger bond. A higher contact angle of greater than 90 degree, on the other hand, means that the fiber is hydrophobic, i.e., it will repel water and hence develop a porous interface, a weaker bond and poor adhesion. In order to strengthen the fiber-matrix bonding, a number of attempts have been made to modify the fiber surface and reduce the contact angle including ozone treatment [16], acid or alkali treatment [17] and plasma treatment [18]. Perceivably, if the contact angle can be reduced by reducing the surface tension of the water in cement paste, it may provide a cost-effective way of improving the fiber-matrix bonding.

SRAs have also shown some negative side effects on concrete properties. It has been observed that addition of SRA to the mix water depresses the dissolution of alkalis in the pore fluid 14 which in some case may delay setting, reduce the rate of cement hydration and impede strength development. By extension, in fiber reinforced concrete, an excessive amount of SRA may under nourish the transition zone between fiber and the matrix, and may, in fact, reduce the strength of the bond.

Combination of fibers and SRA has been used to mitigate cracking potential in concrete and mortar [19, 20]. For example, Hwang et al. [19] suggested that combined use of SRA and synthetic fibers is effective to produce high-performance self-consolidating concrete of low cracking potential. Passuello et al. [20] evaluated crack reduction potential by incorporating SRA in fiber-reinforced concrete. They found out that this combination of SRA and fibers led to better cracking resistance even with reduced dosage of fibers. They attributed this to reduced dry shrinkage cracking by use of SRA and increased resistance to crack opening by fibers. However, so far no paper deals specifically with effect of SRA on surface tension, contact angle, and finally on flexural performance of fiber reinforced concrete.

1.1. Research significance

Incorporation of SRA in mortar or concrete not only reduces surface tension of pore solution, but also reduces contact angle between fiber and mixing water. Both effects may contribute to better fiber-matrix bonding and improved flexural performance, toughness, and residual strength of fiber-reinforced cementitious composites, which would benefit the safety of buildings. However, no previous investigation has considered this possibility. In this study, two types of commercially available macro-fibers—steel fiber (ST) and polypropylene (PP)—were used. The influence of different concentrations of SRA was investigated on the wettability of the fibers and on the flexural performance of the resulting mortars and concretes.

2. Experimental investigation

2.1. Materials

The shrinkage reducing admixture used in this study was Eclipse® Floor which is a commercially available product from W.R. GRACE. According to manufacturer's data sheet, it is a clear liquid admixture without water.

Properties of the steel fiber (ST) and polypropylene (PP) fibers used in this study are given in Table 1 and their pictures are given in Fig. 1. Both mortar (M) and high strength concrete (HSC) were chosen as the matrix. ASTM Type I cement was used throughout. Fine aggregate with a fineness modulus of 2.96 was used both in the mortar and high strength concrete. The coarse aggregate with a size range of 2.36-10mm was used in HSC. Effect of silica fume was investigated and compared with SRA. The chemical compositions of cement and silica fume are given in Table 2.

2.2. Mixture proportions of Mortar (M) and High Strength Concrete (HSC)

The mixture proportions of the cement mortar matrix are given in the Table 3 (Note: ST denotes steel fiber, PP denotes polypropylene fiber, SF denotes silica fume, and SRA_3 means the concentration of SRA by mass of water is 3%). Mixture proportions of mortar are given in terms of mass ratios because of the uncertain air content in these mixes. A fiber volume fraction of 0.5% was chosen and used throughout so that the FRC can attain moderate flexural performance without compromising workability significantly. Thus, effects of various factors on the flexural performance of the FRC can be evaluated. For SRA, three concentration levels of 0%, 3% and 7.14% by mass of water, were chosen for steel fiber reinforced cement mortar and 0%, 3% and 12.5% by mass of water were chosen for PP fiber reinforced cement mortar. The reason for choosing these concentration levels will be discussed later. Although dosages of 2.5 to 5% are recommended by manufacturer, the dosages of 0 to 7.14 and 0 to 12.5% for steel fiber and PP fiber respectively described in this paper were selected for research purposes. Superplasticizer (SP) was changed to control the workability of all mixtures. Measurement of mortar workability complied with BS EN 1015-3 (Flow table Method) [21]. The mixture proportions of HSC are given in Table 4. Water given in Table 3 and Table 4 is the total water in the mix, 60% of SP and 100% SRA by mass were used to replace same mass of water when casting.

2.3. Preparation and Curing of Test Specimens

For each mixture, four 100 x 100 x 400 mm beam specimens and six 100 mm cube specimens were cast by using a vibrating table. Specimens were covered by plastic sheets and demolded 24 h after casting and stored for an additional 27 days under controlled conditions of 28 -30 °C and 100% RH.

2.4. Testing

2.4.1. Surface Tension Measurement with Deionized Water and Synthetic Pore Solution

Deionized water (DIW) and synthetic pore solution (SPS) (0.35 M KOH+0.05 M NaOH in DIW) were chosen as the bulk solution with different concentrations of SRA (by mass of bulk solution). The surface tension of these solutions was measured by using Wilhelmy Plate Method with a K14 Krüss Tensiometer (accuracy 0.01 mN/m) (Krüss, Germany).

2.4.2. Measurement of Contact Angle between Fibers and Synthetic Pore Solution

To simulate the case in which fiber comes in contact with the fresh cement paste, the synthetic pore solution (SPS) was chosen and the contact angle was measured. The same equipment K14 Krüss tensiometer was used for measuring the dynamic contact angle between fiber and SPS. For these measurements, the tension metric method (Micro-Wilhelmy technique) was used [17]. A schematic diagram of this method is given in Fig. 2. The immersion depth was up to 5 mm and the stage with a beaker of SPS was moved up (advancing) and down (receding) at a constant speed of 5 mm/min. At least six samples under each condition and for each fiber type were tested. Since the advancing contact angle is more stable and with a smaller standard deviation, it was chosen to describe the wettability of the fiber in SPS.

2.4.3. Density and Compressive Strength

Density of all specimens was measured after demolding. Air content of mixtures was measured using the gravimetric method as per ASTM C138. Raw materials density used in this method was measured by AccuPyc 1330 Pycnometer which is a gas displacement pycnometer. Compressive strength of every mixture was tested at 7 and 28 days as per BS EN 12390-3:2002 [22].

2.4.4. Flexural Performance

Flexural toughness of 100 x 100 x 400 mm specimens was measured under third-point loading (four-point bending) using an Instron closed-loop, servocontrolled test system as per ASTM C1609 [23]. Photograph of the test setup is given in Fig. 3. During a test, both the applied load and the mid-span deflection of the specimen in the direction of the applied load were recorded. The deflections were measured by two linear variable displacement transducers (LVDTs) placed on both sides of the specimen and the results from which were averaged as the feed-back signal to the servo-valve. The outcome of this test is in the form of a load-versus-deflection curve from which flexural toughness parameters are derived using absolute values of load or strength at specific deflections. Four specimens were tested for each mixture, and the flexural load-versus-deflection curves were averaged using the software Origin 7.5.

The parameters derived from ASTM C1609 are given as below：

L=Span length (300mm in our case)

P_P=Peak load

ä$_P$=Net deflection at Peak Load

f_p=Peak strength or modulus of rupture (MOR)

P_{600}^{D}**=Residual Load at net deflection of L/600** (0.5mm in our case)

f_{600}^{D}**=Residual Strength at net deflection of L/600**

P_{150}^{D}**=Residual Load at net deflection of L/150** (2mm in our case)

f_{150}^{D}**=Residual Strength at net deflection of L/150**

T_{150}^{D}**=Area under the load vs. net deflection curve 0 to L/150**

D=nominal depth of the beam specimen in mm (100 mm in our case)

FT=Flexural toughness factor from JSCE SF-4

The load-deflection curves can also be analyzed for the Flexural Toughness Factor (FT) as per JSCE SF-4 [4,24] and the Post-Crack Strength (PCS) values as suggested by Banthia [25]. The JSCE SF-4 equation for flexural toughness factor (FT) is:

$$FT = \frac{T_{150}^{D} L}{(L/150) b h^2} \quad (1)$$

where L is the span (300 mm in our case) and b and h are width and depth of the specimen (both 100 mm in our case). It can be seen that FT is a linear function of T_{150}^{D}. Therefore, either of these two parameters can be used to characterize the toughness at a net deflection of L/150. In this study, ASTM C1609 and JSCE SF-4 were chosen for characterization of flexural toughness.

3. Results and discussion

3.1. Surface Tension of Deionized Water and Synthetic Pore Solution

Test results of surface tension are plotted in Fig. 4. From Fig. 4, a steep reduction in the surface tension is observed with the addition of SRA at lower concentrations. Beyond a critical concentration, however, further addition of SRA does not significantly reduce the surface tension. The critical concentration of SRA is roughly around 7.14% for deionized water (DIW) and close to 3% for synthetic pore solution (SPS).

3.2. Contact Angle between Fibers and Synthetic Pore Solution

Test results of advancing contact angle are plotted in Fig. 5. Notice that there is a steep drop in the contact angle due to SRA and there are critical concentrations beyond which an increase in the SRA concentration does not reduce the contact angle any further. This value, however, is much larger for PP fiber (close to 12.5%) than that for steel fiber (close to 7.14%). That is why range of 0 to 7.14% and 0 to 12.5% of SRA concentrations are chosen for steel fiber and PP fiber respectively.

3.3. Effect of SRA on the Density and Compressive Strength of Mortar and Concrete

Properties of hardened mortars and concretes, including compressive strength, hardened density and air content (calculated by gravimetric method) of all mixtures, are given in Table 5. Hardened density and air content are correlative parameters which relate to the compactability of the mixtures.

It can be seen from Table 5 that among the mixes with no SRA, ST-SRA_0 had much larger air content than PP-SRA_0, probably because steel fiber used in this study has a much smaller equivalent diameter than PP fiber, which meant a larger specific surface area. In addition, steel fibers are also much stiffer than PP fiber thus causing a general lack of mobility in mixes with steel fibers and a reduced ability for the entrapped air to escape.

For fiber reinforced mortars, the results of air content and compressive strength versus concentration of SRA are plotted in Fig. 6 (a) and (b). It can be observed that an increase in the concentration of SRA sharply reduced the air content when the SRA content was increased from 0% to 3%, but only a marginal further reduction occurred from 3% to 7.14%

for steel fiber and from 3% to 12.5% for the PP fiber. When Fig. 6 is compared with Fig. 4 and Fig. 5, it may be noted that that the air content of mortar is related to the contact angle of fiber and the surface tension of the emulsion of SRA in SPS. A reduction in the surface tension of the mix water thus enables the air bubbles to collapse in the mix and be removed during the process of compaction.

It is well known that a reduction in air content will improve the mechanical properties of mortar [13]. This appears to be the case here, but as seen in Fig. 6 (a) and (b), after a steep increase in the compressive strength when the SRA content is increased from 0% to 3%, a further increases in the SRA content although decreased the air, there is, in fact, a drop in the compressive strength. This is likely due to the negative effects of SRA as discussed previously. SRA, as indicated, impedes the dissolution of alkalis in the pore fluid [14] and thus reduces the rate of cement hydration and strength gain. When SRA is compared with silica fume, (comparing **ST-SRA_0** and **ST-SF+SRA_0**, or **ST-SRA_7.14** and **ST-SF+SRA_7.14**, Table 5), it appears that although an addition of silica fume can improve the compressive strength, it has little effect on either the air content or the hardened density.

Contrary to the cement mortar, data in Table 5 indicate that SRA doesn't have a significant effect on either the hardened density or the air content of HSC. It appears that the presence of coarse aggregate allows the air to escape even in the absence of SRA and the presence of SRA is only harmful that leads to a 10 MPa drop in the compressive strength (from **HSC-SRA_0** to **HSC-SRA_3**).

3.4. Flexural Performance

Load deflection curves of all mixtures are plotted in Fig. 7 to Fig. 10. The flexural toughness parameters as derived from these curves according to ASTM C1609 and JSCE SF-4 are summarized in Table 6.

3.4.1. Fiber Reinforced Mortar

Fig. 7 shows the comparison of steel fiber reinforced cement mortar with different dosages of SRA. Fig. 8 shows the comparison of PP fiber reinforced cement mortar with different dosages of SRA. FT values of cement mortar reinforced with different fibers are plotted in Fig. 11. As shown in Fig. 7 and Fig. 8, fiber reinforced cement mortars with 3% of SRA (**ST-SRA_3** and **PP-SRA_3**) demonstrated the best flexural behavior among the three SRA concentrations investigated. By comparing Fig. 11 with Fig. 6, it can be observed that the trend of FT versus SRA concentration is the same as that of compressive strength versus SRA concentration. FT of **ST-SRA_3** is higher than **ST-SRA_0** by almost 52%. However, with a further increase of SRA to 7.14% by concentration, the toughness improved only by 21% compared with **ST-SRA_0** but actually decreased by about 20% over **ST-SRA_3**. In the case of PP fiber, a similar trend is noticed (Fig. 8) but the increase from 0 to 3% of SRA is smaller than that for steel fiber and at 12.5% (**PP-SRA_12.5**), FT drops even below that of the control with no SRA (**PP-SRA_0).** The FT value of **PP-SRA_12.5** is just 64% of that of **PP-SRA_0**.

In these tests, although SRA, which is a pure organic chemical, is replacing the mix water by its own mass and a marginal reduction in the water to cement ratio is taking place, this is not benefiting the mechanical properties of mortar at higher SRA dosages.

It is also meaningful to notice that the numerical improvements in the FT values due to SRA addition for PP fiber are not as significant as they are for the steel fiber. The improvement in FT for PP fiber (comparing **PP-SRA_0** to **PP-SRA_3)** is around 0.5 MPa, whereas that for the steel fiber is around 2 MPa (comparing **ST-SRA_0** to **ST-SRA_3)**.

MOR of all mixtures is also presented in Table 6. For steel fiber reinforced cement mortar, the trend of MOR verse SRA concentration is the same as that for compressive strength and

FT. However, for PP fiber reinforced cement mortar, MOR keeps reducing from **PP-SRA_0** to **PP-SRA_12.5**, in spite of a reducing air content.

From the discussion above, it can be concluded that there is an optimal SRA concentration for application in cement mortars. SRA, at this optimal concentration can achieve a balance between the positive effects such as reductions in the air content and the fiber contact angle and the negative effects such as a reduced hydration rate and strength gain [26]. According to the test results in this study, the critical SRA concentration is around 3% by mass of water, which is within the recommended dosage rate (from 2.5% to 5.0%) given by the manufacturer.

Influence of silica fume on the flexural toughness properties of steel fiber reinforced cement mortar in the presence or absence of SRA is considered in Fig. 9. Curves without SRA are plotted in Fig. 9 (a) and curves for an SRA content of 7.14% by mass of water are given in Fig. 9 (b). It can be observed that the addition of silica fume significantly improves the peak strength (MOR) of steel fiber reinforced mortar. By comparison of **ST-SRA_0** and **ST-SF+SRA_0**, or **ST-SRA_7.14** and **ST-SF+SRA_7.14** (Table 6), an improvement in the MOR due to silica fume addition of 1 MPa without SRA and 1.2 MPa with SRA can be noted. These effects are entirely attributable to silica fume as the air content of these two groups is quite similar. One can also notice that an addition of silica fume only marginally improves the post-peak behavior. The differences in f_{600}^{D} between **ST-SRA_0** and **ST-SF+SRA_0**, or **ST-SRA_7.14** and **ST-SF+SRA_7.14**, are only of 0.31MPa and 0.58 MPa, respectively. As single fiber pull-out tests have shown [11], silica fume may enhance the bond, but may also promote post-crack brittleness and this may somewhat compromise the toughness again. Some synergy between silica fume and SRA may also be noted. When T_{150}^{D}, values are considered, mortar with both SRA and silica fume (**ST-SF+SRA_7.14**) achieved a greater benefit over the control **ST-SRA_0** as compared to SRA alone (**ST- SRA_7.14)** or silica fume alone (**ST-SF+SRA_0)**.

According to the discussion above, 3% of SRA by mass can increase the flexural toughness factor of steel fiber reinforced mortar by 52%. In other words, to achieve the same flexural toughness, volume fraction of steel fibers can be reduced with the incorporation of SRA. In addition, the residual strength f_{150}^{100} at net deflection of 1/150 of the span length of the mortar with 3% SRA (**ST-SRA_3)** was increased by 51% compared with **ST-SRA_3**.

3.4.2. Steel Fiber Reinforced High Strength Concrete

Comparison of steel fiber reinforced HSC with different dosages of SRA is given in Fig. 10. As seen in Fig. 10 and in Table 6, although the presence of SRA does not change the MOR much, there is actually a slight drop in the post-peak performance and a reduction of around 2.95J in the T_{150}^{D} values. This observation can be attributed to the fact that the addition of SRA doesn't alter the air content, but creates a somewhat undernourished transition zone between fiber and matrix due to the negative effects of SRA [14,26].

For steel fiber, the influence of matrix (mortar or concrete) on the flexural toughness is shown in Fig. 12. One can notice that a mortar matrix (**ST-SRA_3**) has a stronger flexural performance than the concrete matrix (**HSC-SRA_3)**; T_{150}^{D} of **ST-SRA_3** is almost 33% higher than that of **HSC-SRA_3**. While mortars may not be applied in all applications due to cost and sustainability concerns, this observation may be particularly relevance for thin sheet applications, for repair overlays and for dry-process shotcrete.

4. Conclusions

Based on the results of this experimental investigation, the following conclusions are drawn:

1. Shrinkage reducing admixture (SRA) reduces the surface tension of both deionized water and synthetic pore solution and also reduces the contact angle that steel and polypropylene fibers developed with the synthetic pore solution. SRA thus enhances the wettability of fibers. There are, however, critical SRA concentrations beyond which there is little effect either on the surface tension or on the contact angle.
2. SRA reduces the air content of fiber reinforced cement mortars. There exists a critical concentration at which this effect is maximized. Beyond this concentration, there is only a marginal benefit of SRA addition.
3. The addition of SRA can significantly improve the mechanical properties, specifically the flexural toughness, of the steel reinforced mortar. A 3% concentration of SRA by mass of water can improve the flexural toughness factor of steel fiber reinforced mortar by 52% and increase residual strength by 51%. Beyond 3%, however, the benefits are only marginal.
4. In the case of PP fiber, SRA is not as effective in enhancing the flexural toughness as it is in the case of steel fiber.
5. SRA doesn't significantly reduce the air content of High Strength Concrete (HSC) and the negative effects of SRA are more dominant. The properties of steel fiber reinforced HSC with SRA are inferior to those of steel fiber reinforced HSC without SRA. Thus, cement mortar is a more suitable matrix in SRA modified fiber reinforced cementititous composites. This conclusion is of particular relevance for thin sheet applications, for repair overlays and for dry-process shotcrete.

Acknowledgement

Grateful acknowledgement is made to A*STAR (project no. 0921420044) for funding this research.

References

[1] American Concrete Institute (ACI) Committee 544. State-of-the-art report on fiber reinforced concrete. Concrete international: Design and construction, 544.IR-82, Detroit, 1982, pp. 9–30.

[2] American Concrete Institute (ACI) Committee 544. Guide for Specifying, Proportioning, and Production of Fiber Reinforced Concrete. American Concrete Institute, 544.3R-08, Farmington Hills, USA, pp. 12.

[3] American Concrete Institute (ACI) Committee 544. Report on the Physical Properties and Durability of Fiber Reinforced Concrete. American Concrete Institute, 544.5R-10, Farmington Hills, USA, pp. 31.

[4] Nataraja MC, Dhang N, Gupta AP. Toughness characterization of steel fiber-reinforced concrete by JSCE approach. Cem Concr Res 2000;30(4):593-597.

[5] Gokoz UN, Naaman AE. Effect of strain-rate on the pull-out behaviour of fibres in mortar. Int J Cem Compos Lightweight Concr 1981;3(3):187-202.

[6] Banthia N, Trottier JF. Micromechanics of steel fiber pull-out: rate sensitivity at very low temperatures. Cem Concr Compos, Special Issue on Micromechanics of Failure in Cementitious Composites 1992;14(2):119-130.

[7] Naaman AE, Shah SP. Pull-Out Mechanism in Steel Fiber-Reinforced Concrete. ASCE Journal of the Structural Division 1976;102(8):1537-1548.

[8] Al KM, Page CL, Ritchie AG. Effects of fibre surface composition on mechanical properties of steel fibre reinforced mortars. Cem Concr Res 1980;10(1):71-77.

[9] Mayfield B, Zelly BM. Steel fiber treatment to improve bonds. Concrete 1973;7(3):35-37.

[10] Banthia N, Yan C. Bond-slip characteristics of steel fibers in high reactivity metakaolin (HRM) modified cement-based matrices. Cem Concr Res 1996;26(5):657-662.

[11] Banthia N. A study of some factors affecting the fiber–matrix bond in steel fiber reinforced concrete. Can J Civil Eng 1990;17(4):610-620.

[12] P. Kumar Mehta, and Paulo J. M. Monteiro. Concrete, microstructures, properties, and materials. Third Edition. New Jersey, USA: Prentice-Hall, 2006, pp. 511.

[13] Pierre P, Pleau R, Pigeon M. Mechanical properties of steel microfiber reinforced cement pastes and mortars. J Mater Civil Eng 1999;11(4):317-324.

[14] Rajabipour F, Sant G, Weiss J. Interactions between shrinkage reducing admixtures (SRA) and cement paste's pore solution. Cem Concr Res 2008;38(5):606-615.

[15] Chan YW, Li VC. Effects of transition zone densification on fiber/cement paste bond strength improvement. Adv Cem Based Mater 1997;5(1):8-17.

[16] Fu X, Lu W, Chung DD. Ozone treatment of carbon fiber for reinforcing cement. Carbon 1998;36(9):1337-1345.

[17] Lu W, Fu X, Chung DD. A comparative study of the wettability of steel, carbon, and polyethylene fibers by water. Cem Concr Res 1998;28(6):783-786.

[18] Felekoglu B, Tosun K, Baradan B. A comparative study on the flexural performance of plasma treated polypropylene fiber reinforced cementitious composites. J Mater Process Tech 2009;209(11):5133-5144.

[19] Hwang SD, Khayat KH. Effect of mixture composition on restrained shrinkage cracking of self-consolidating concrete used in repair. ACI Mater J 2008;105(5):499-509.

[20] Passuello A, Moriconi G, Shah SP. Cracking behavior of concrete with shrinkage reducing admixtures and PVA fibers. Cem Concr Compos 2009;31(10):699-704.

[21] BS EN 1015-3:1999. Methods of test for mortar for masonry: Determination of

consistence of fresh mortar (by flow table). pp. 10.

[22] BS EN 12390-3:2002. Testing hardened concrete. Compressive strength of test specimens. pp. 18

[23] ASTM C1609 / C1609M-07. Standard Test Method for Flexural Performance of Fiber-Reinforced Concrete (Using Beam With Third-Point Loading). American Society of Testing and Materials, 2007, pp. 1-8.

[24] JSCE SF-4. Method of test for flexural strength and flexural toughness of fiber reinforced concrete (SF-4). Japan Society of Civil Engineers, Tokyo, 1984, pp. 58–66.

[25] Banthia N, Trottier JF. Test methods for flexural toughness characterization of fiber reinforced concrete: Some concerns and proposition. ACI Mater J 1995;92(1):146-156.

[26] Folliard KJ, Berke NS. Properties of high-performance concrete containing shrinkage-reducing admixture. Cem Concr Res 1997;27(9):1357-1364.

TABLES

List of Tables:

Table 1 –Properties of fibers

Fiber types	Tensile strength (MPa)	Elastic modulus (GPa)	Length (mm)	Diameter (μm)	Aspect ratio	Geometry
Steel	2500	200	13	160	81	Straight
Polypro-pylene (PP)	620	9.5	40	444	90	Straight

Table 2 –Chemical and mineral compositions of cement and silica fume

Chemical Composition (%)	CaO	SiO_2	Al_2O_3	Fe_2O_3	MgO	Na_2O	K_2O	SO_3	LOI	C_3S	C_2S	C_3A	C_4AF
Cement	63.6	21.6	4.2	3.0	2.4	0.19	0.5	2.7	2.2	54.1	24.8	7.5	7.5
Silica fume	0.2	96.0	0.3	0.3	0.4	0.05	0.6	0.2	1.5	N/A	N/A	N/A	N/A

Table 3 –Mix proportion of mortar (M) matrix

Fiber Type	Fiber Dosage	Mix ID	Water	Cement	Silica fume	Sand	Super-plasticizer (%)[a]	SRA (%)[a]	SRA (%)[b]	Flow (mm)
ST	0.5%	ST-SRA_0	0.45	1	0	2.5	0.86	0	0	196
		ST-SRA_3	0.45	1	0	2.5	0.9	1.35	3	196
		ST-SRA_7.14	0.45	1	0	2.5	0.95	3.2	7.14	228
		ST-SF+SRA_0	0.45	0.92	0.08	2.5	0.9	0	0	215
		ST-SF+SRA_7.14	0.45	0.92	0.08	2.5	1.05	3.2	7.14	198
PP		PP-SRA_0	0.45	1	0	2.5	0.815	0	0	240
		PP-SRA_3	0.45	1	0	2.5	0.815	1.35	3	196
		PP-SRA_12.5	0.45	1	0	2.5	0.815	5.63	12.5	220

[a] By mass of (cement + silica fume)
[b] By mass of water

Table 4 –Mix proportion of high strength concrete (HSC) matrix

Fiber Type	Fiber Dosage	Mix ID	Water (kg/m^3)	Cement (kg/m^3)	Sand (kg/m^3)	Coarse Aggregate (kg/m^3)	Super-plasticizer (L/m^3)	SRA (kg/m^3)	Vebe time (s)
ST	0.5%	HSC-SRA_0	180	500	748	952	6	0	5
		HSC-SRA_3	180	500	748	952	6	5.4	4

Table 5 –Test results: compressive strength, hardened density and air content

Mixture Type		Mix ID	Compressive strength (MPa)	Hardened density (kg/m^3)	Air content (%)
Mortar (M)	Steel Fiber	ST-SRA_0	50.0	2078	11.6
		ST-SRA_3	64.9	2293	2.3
		ST-SRA_7.14	63.1	2322	1.1
		ST-SF+SRA_0	54.3	2076	11.2
		ST-SF+SRA_7.14	72.7	2285	2.2
	PP Fiber	PP-SRA_0	54.4	2157	6.7
		PP-SRA_3	59.4	2248	2.8
		PP-SRA_12.5	51.4	2275	1.6
High Strength Concrete (HSC)		HSC-SRA_0	94.8	2447	0.98
		HSC-SRA_3	84.0	2436	1.45

Table 6 –Measured toughness parameters from ASTM C1609 Test

	P_p (kN)	δ_p (mm)	f_p *(MOR)* (MPa)	P_{600}^{100} (kN)	f_{600}^{100} (MPa)	P_{150}^{100} (kN)	f_{150}^{100} (MPa)	T_{150}^{100} (J)	*FT* (MPa)
ST-SRA_0	19.91	0.042	5.97	13.35	4.00	10.47	3.14	25.16	3.77
ST-SRA_3	23.90	0.034	7.17	21.16	6.35	15.77	4.73	38.09	5.71
ST-SRA_7.14	22.41	0.032	6.72	16.25	4.87	12.73	3.82	30.54	4.58
ST-SF+SRA_0	23.19	0.042	6.96	14.38	4.31	11.26	3.38	27.28	4.09
ST-SF+SRA_7.14	26.44	0.038	7.93	18.17	5.45	15.10	4.53	34.94	5.24
PP-SRA_0	20.73	0.035	6.22	8.23	2.47	10.30	3.09	19.69	2.95
PP-SRA_3	19.54	0.030	5.86	9.52	2.86	13.15	3.95	22.87	3.43
PP-SRA_12.5	18.69	0.030	5.61	4.67	1.40	6.41	1.92	12.55	1.88
HSC-SRA_0	26.21	0.041	7.86	17.89	5.37	11.83	3.55	31.48	4.72
HSC-SRA_3	26.36	0.047	7.91	15.65	4.69	11.02	3.30	28.54	4.28

List of Figures:

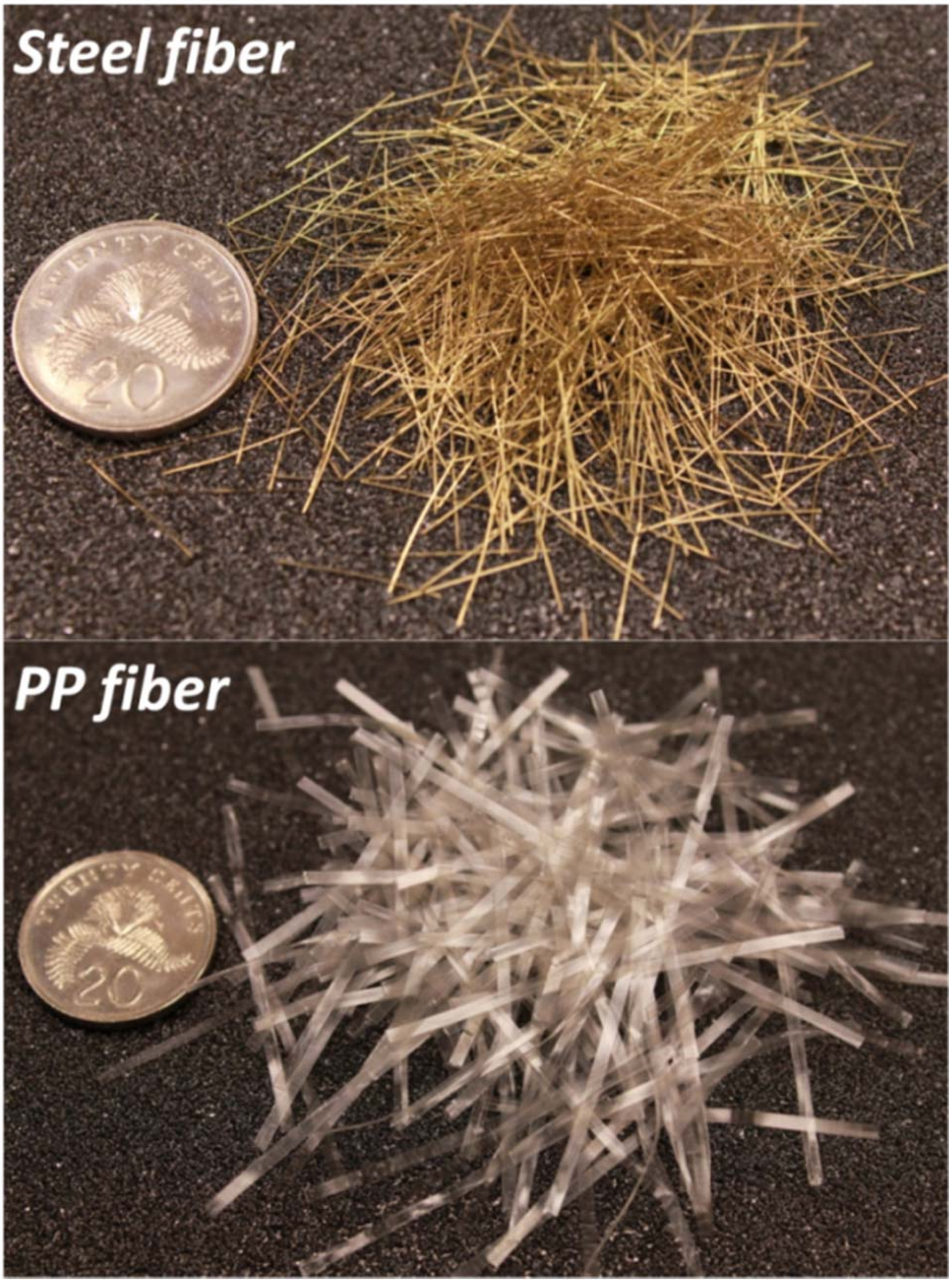

Fig. 1. Pictures of fibers

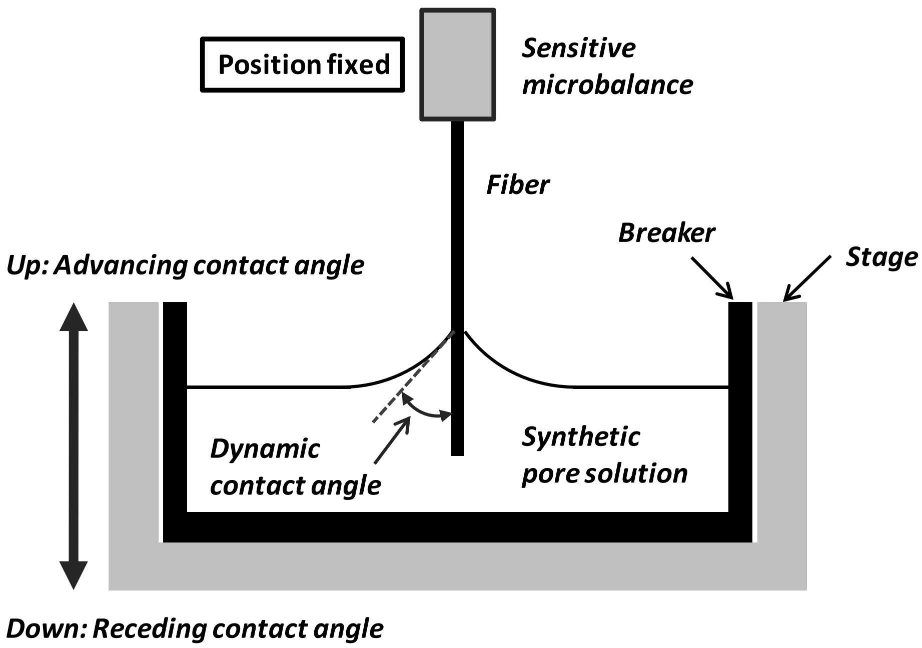

Fig. 2. Schematic diagram of Micro-Wilhelmy technique.

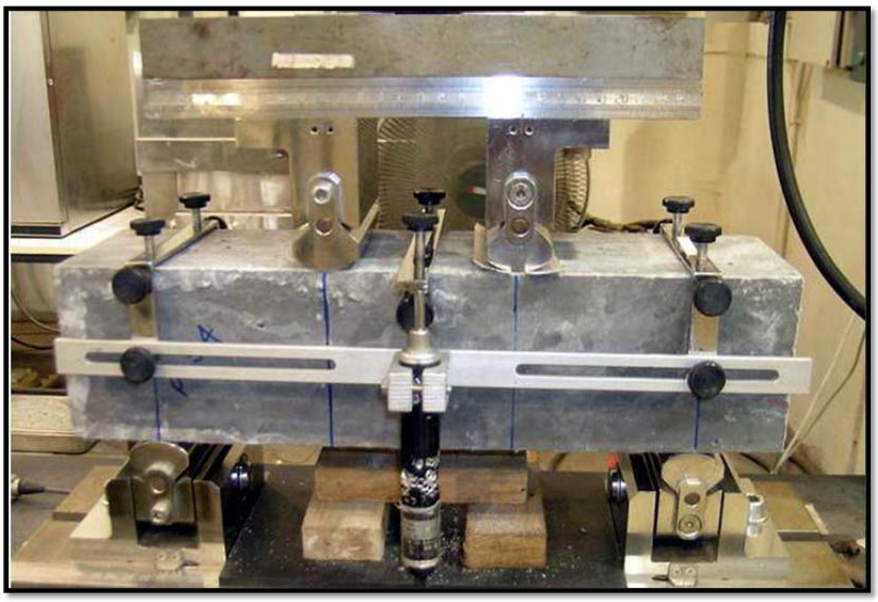

Fig. 3. Photograph of the ASTM C1609 test setup.

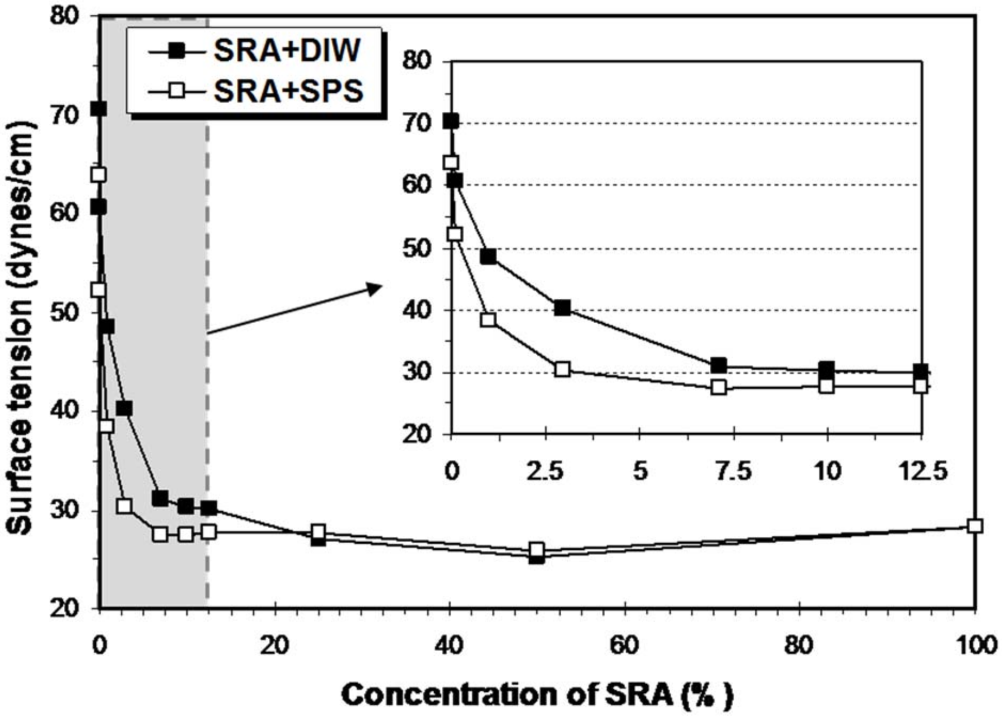

Fig. 4. Surface tension vs. concentration of SRA.

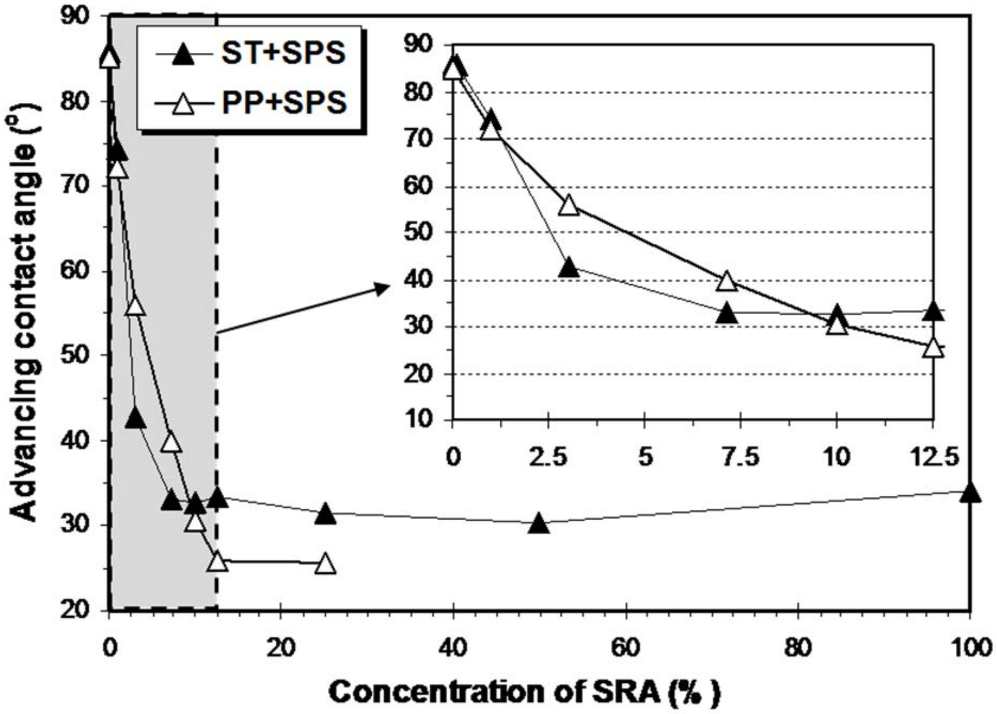

Fig. 5. Advancing contact angle vs. SRA concentration for steel (ST) and polypropylene (PP) Fibers.

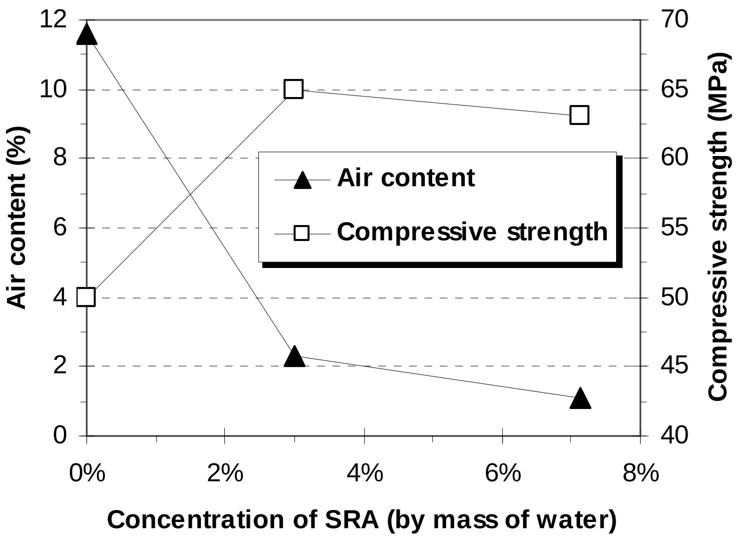

(a) Steel Fiber Reinforced Mortar

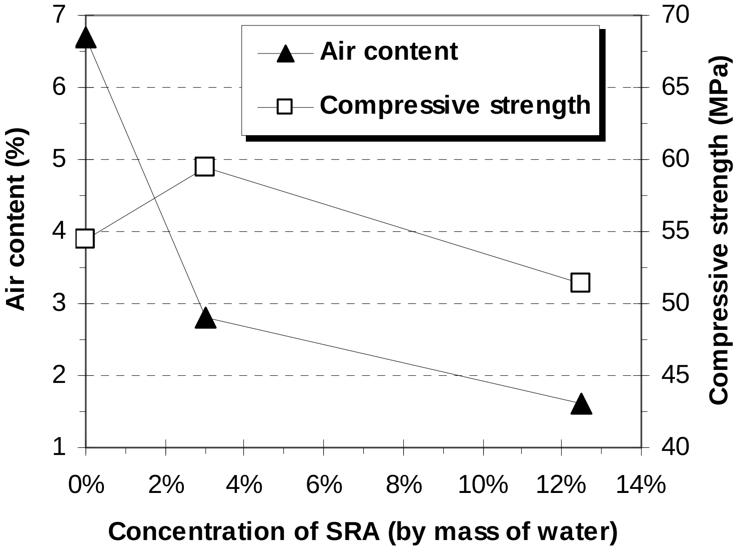

(b) PP Fiber Reinforced Mortar

Fig. 6. Effect of SRA on air content and compressive strength of fiber reinforced mortar: (a) steel fiber reinforced mortar; (b) PP fiber reinforced mortar.

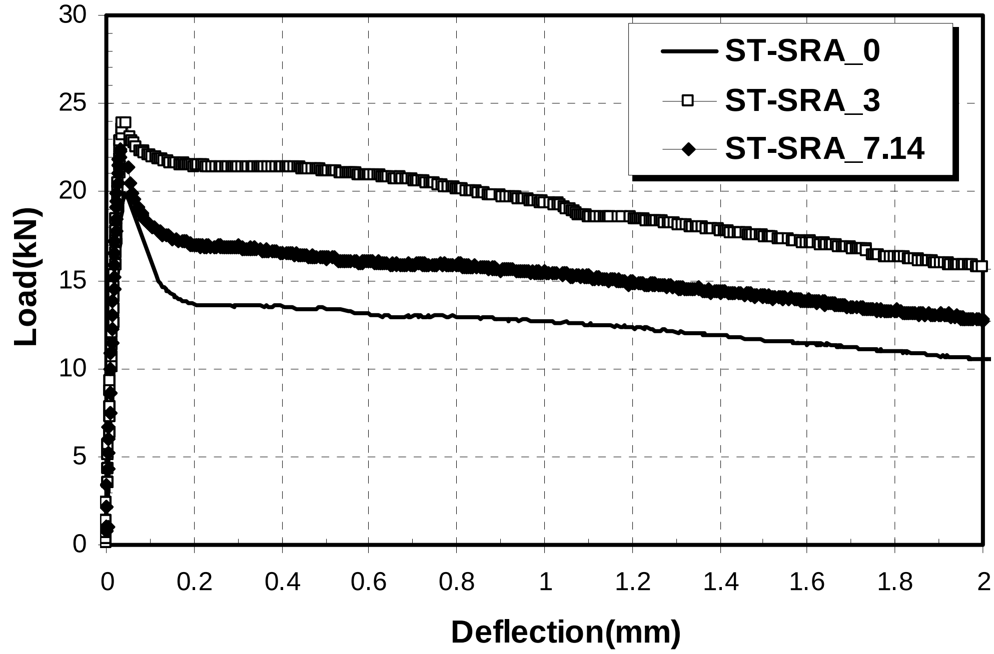

Fig. 7. Comparison of steel fiber reinforced mortar at different dosages of SRA.

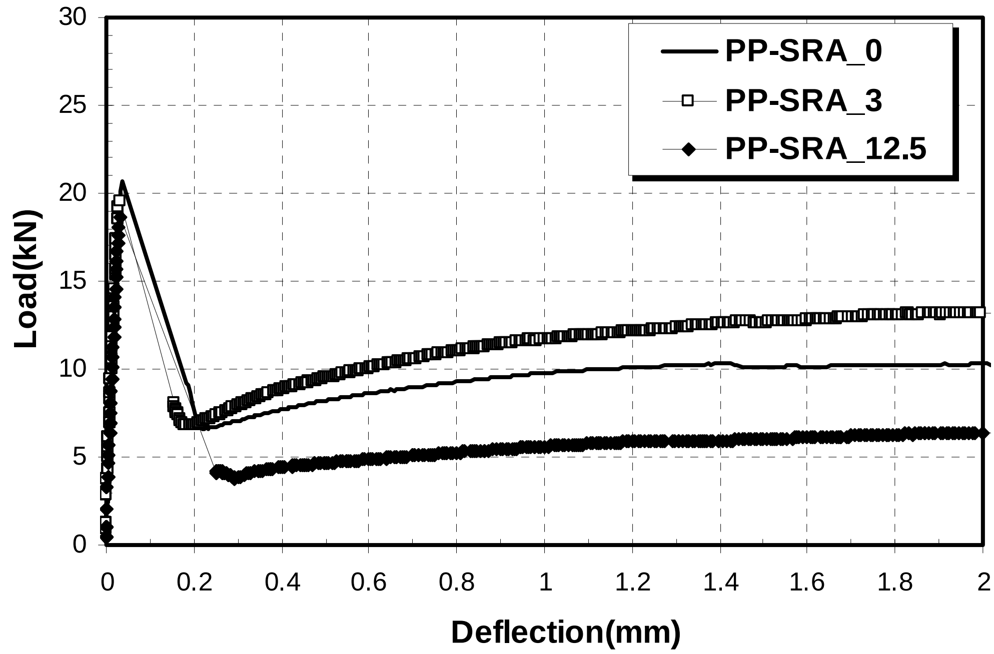

Fig. 8. Comparison of PP fiber reinforced mortar at different dosages of SRA.

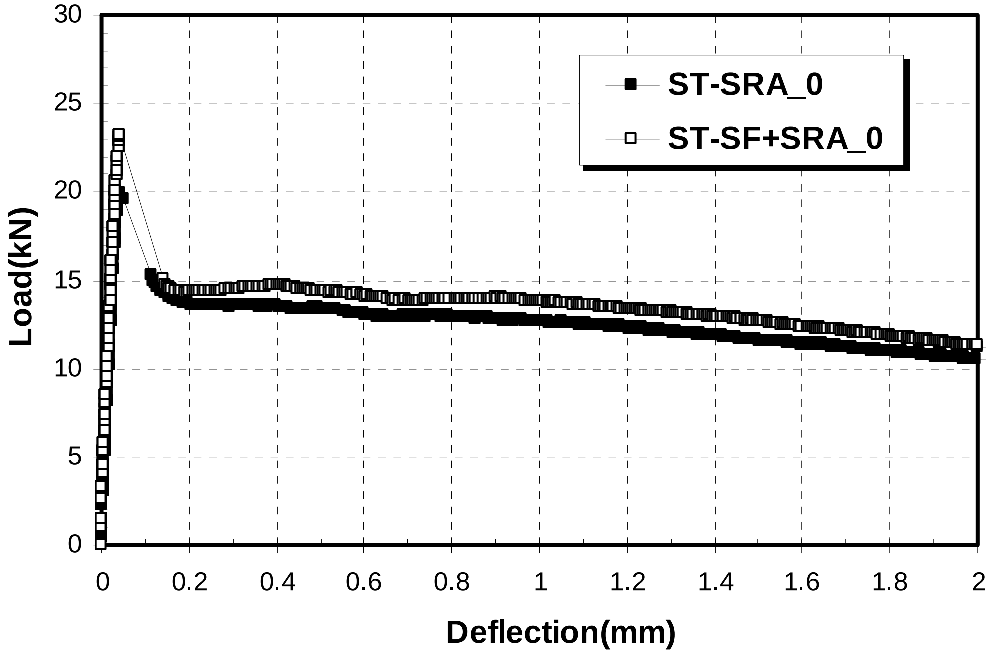

(a) Without SRA

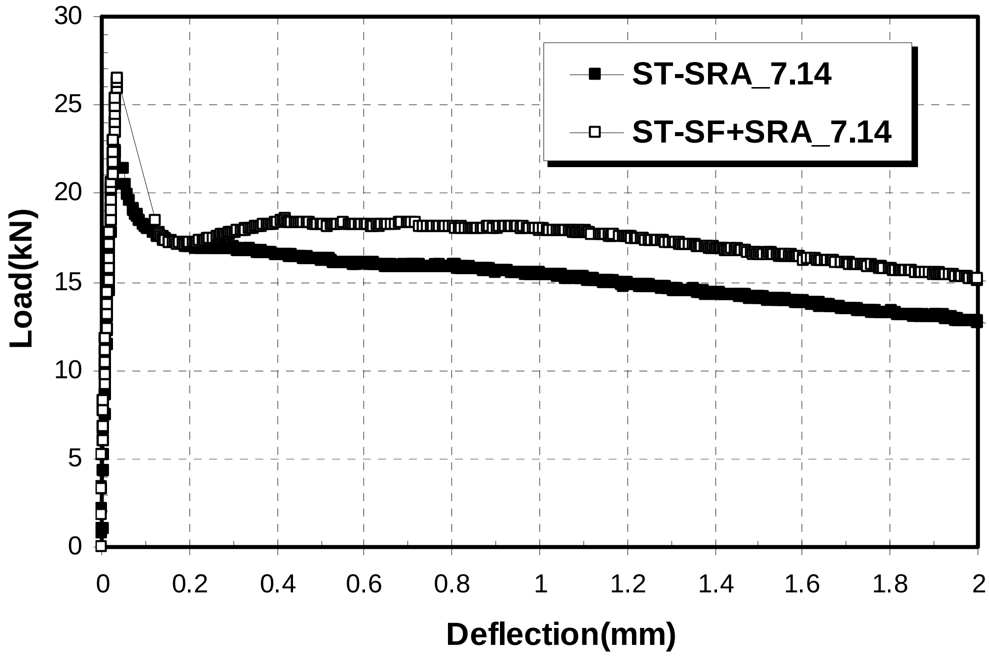

(b) With SRA 7.14% of Water by Mass

Fig. 9. Comparison of steel fiber reinforced mortar with and without silica fume: (a) without SRA; and (b) with SRA (7.14% of water by mass).

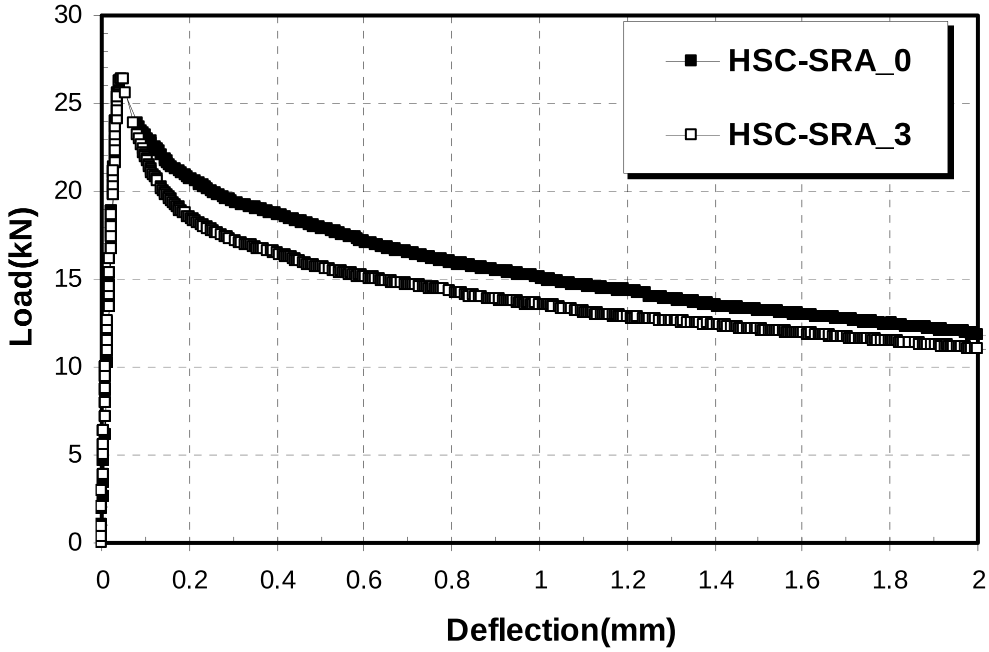

Fig. 10. Comparison of steel fiber reinforced HSC with different dosages of SRA.

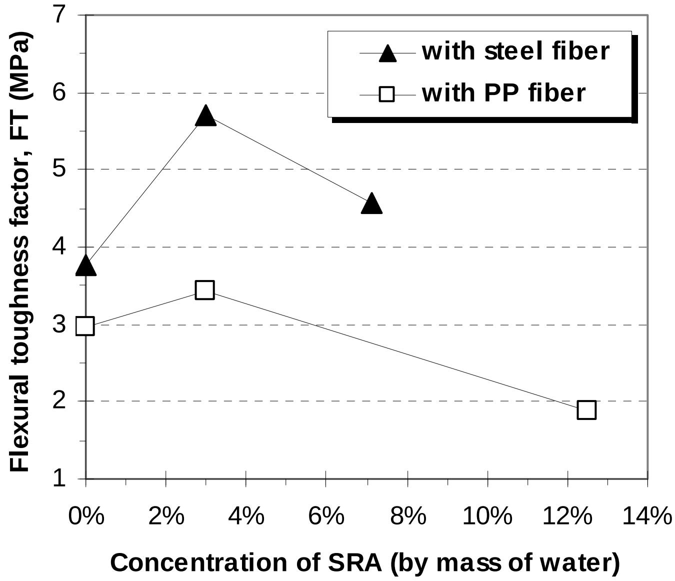

Fig. 11. Flexural toughness factors (FT) for cement mortar reinforced with different fibers.

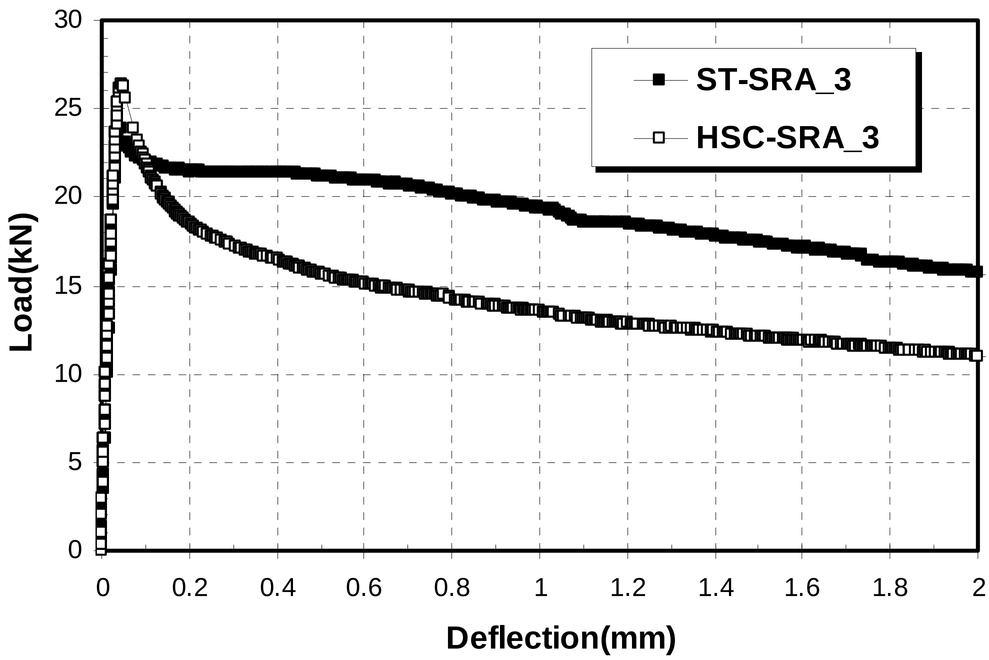

Fig. 12–Comparison of steel fiber reinforced mortar with steel fiber reinforced high strength concrete both carrying 3% SRA